



**10th International Conference on Large Scale Applications
and Radiation Hardness of Semiconductor Detectors**

Offline calibration and performance of the ATLAS Pixel Detector

Attilio Andreazza
INFN and Università di Milano
for the ATLAS Collaboration

- The ATLAS Pixel Detector
- Efficiency
- Resolution
- Detector properties
 - Lorentz angle
 - Energy loss measurement

...and what you do with all that

No alignment and tracking performance

S. Marti's talk later today

No radiation damage issue

S. Gibson's talk on Friday



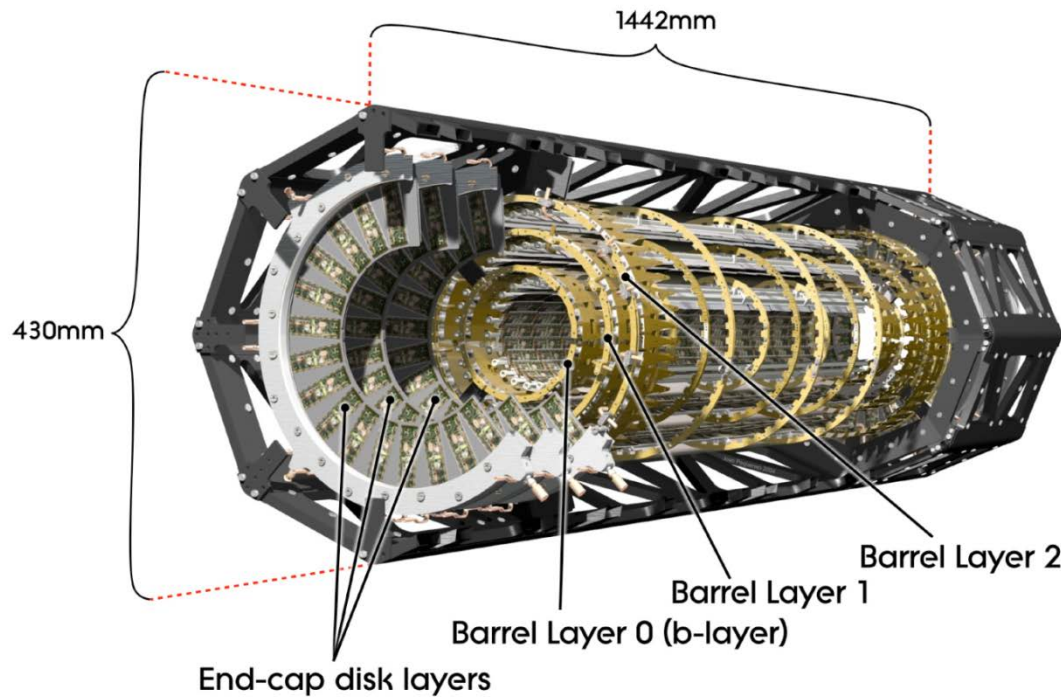
Introduction:

- Pixel Detector layout
- Module concept

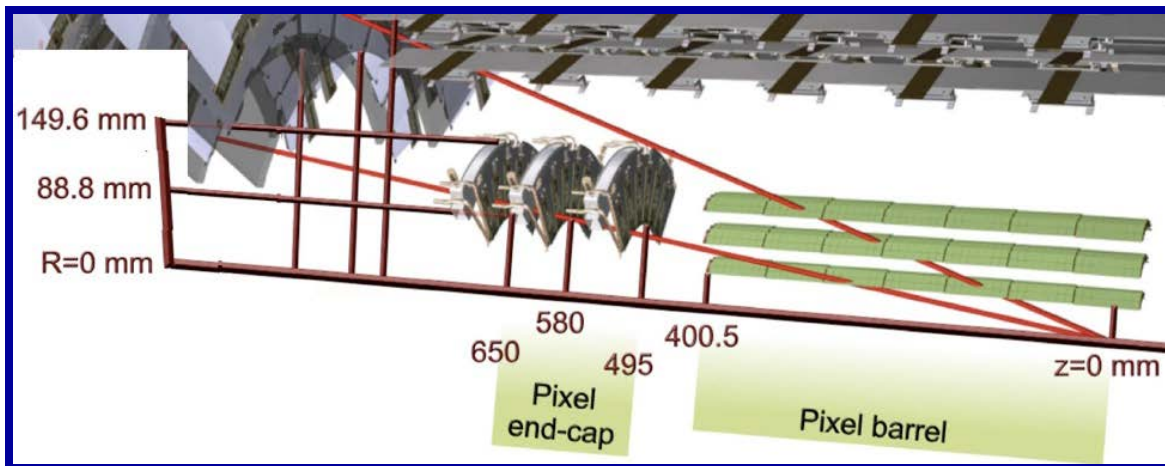
THE ATLAS PIXEL DETECTOR



The ATLAS Pixel Detector



- **Three barrel layers:**
 - R= 5 cm (Layer-0), 9 cm (Layer-1), 12 cm (Layer-2)
 - modules tilted by 20° in the $R\phi$ plane to overcompensate the Lorentz angle.
- **Two endcaps:**
 - three disks each
 - 48 modules/disk
- **Three precise measurement points up to $|\eta| < 2.5$:**
 - $R\Phi$ resolution: $10 \mu\text{m}$
 - η (R or z) resolution: $115 \mu\text{m}$
- 1456 barrel modules and 288 forward modules, for a total of 80 million channels and a sensitive area of 1.7 m^2 .
 - Environmental temperature about -13°C
 - 2 T solenoidal magnetic field.





Module overview

- **Sensor**

- 47232 n-on-n pixels with moderated p-spray insulation
- 250 μm thickness
- 50 μm ($R\Phi$) \times 400 μm (η)
- 328 rows (x_{local})
 \times 144 columns (y_{local})

- **16 FE chips**

- bump bonded to sensor

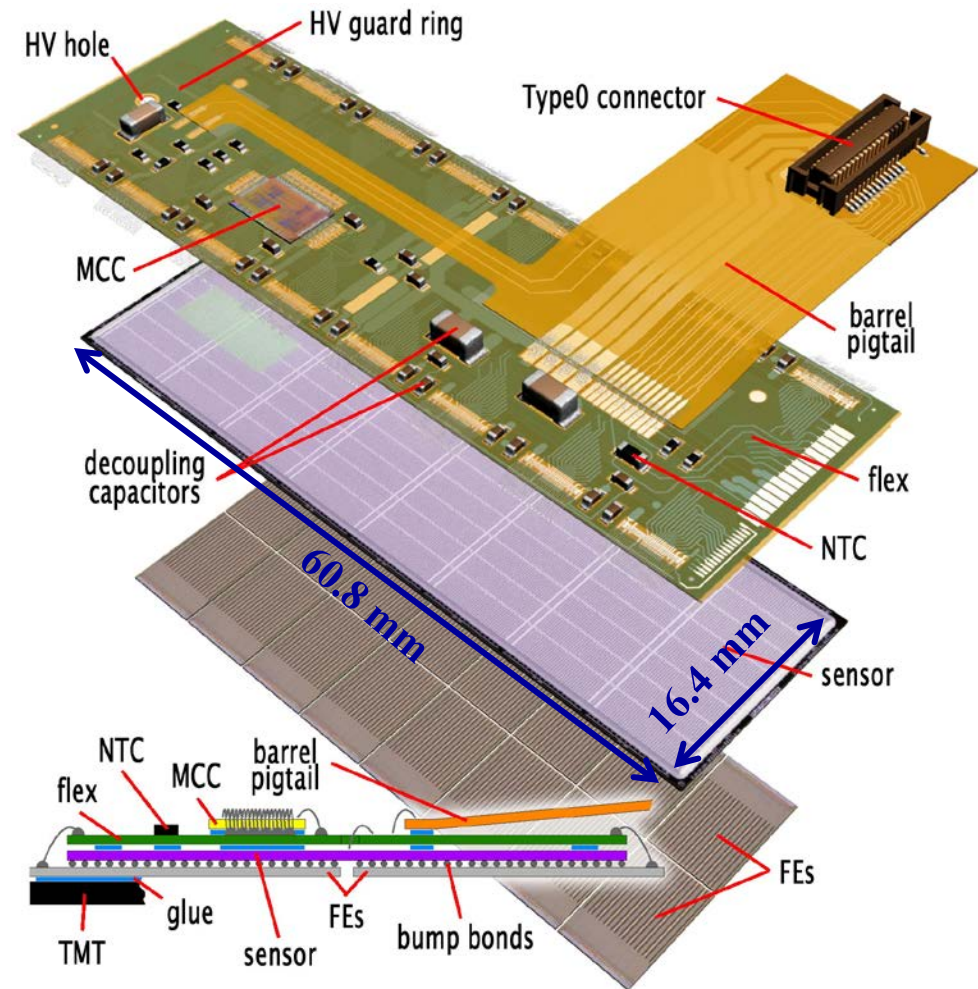
- **Flex Hybrid**

- passive components
- Module Controller Chip to perform distribution of commands and event building.

- **Radiation-hard design:**

- Dose 500 Gy
- NIEL 10^{15} $n_{\text{eq}}/\text{cm}^2$ fluence

5 years at 10^{34} $\text{cm}^{-2}\text{s}^{-1}$





Mapping the detector

- Noise maps
- Inefficiency maps

Putting all in MC and use it reconstruction (p - p and Pb-Pb)

EFFICIENCY



Offline calibration

• “Calibration loop”

- first pass reconstruction of a subset of physics and calibration data
- calibration

- noise maps (per fill)
- dead channels (~monthly)
- charge sharing

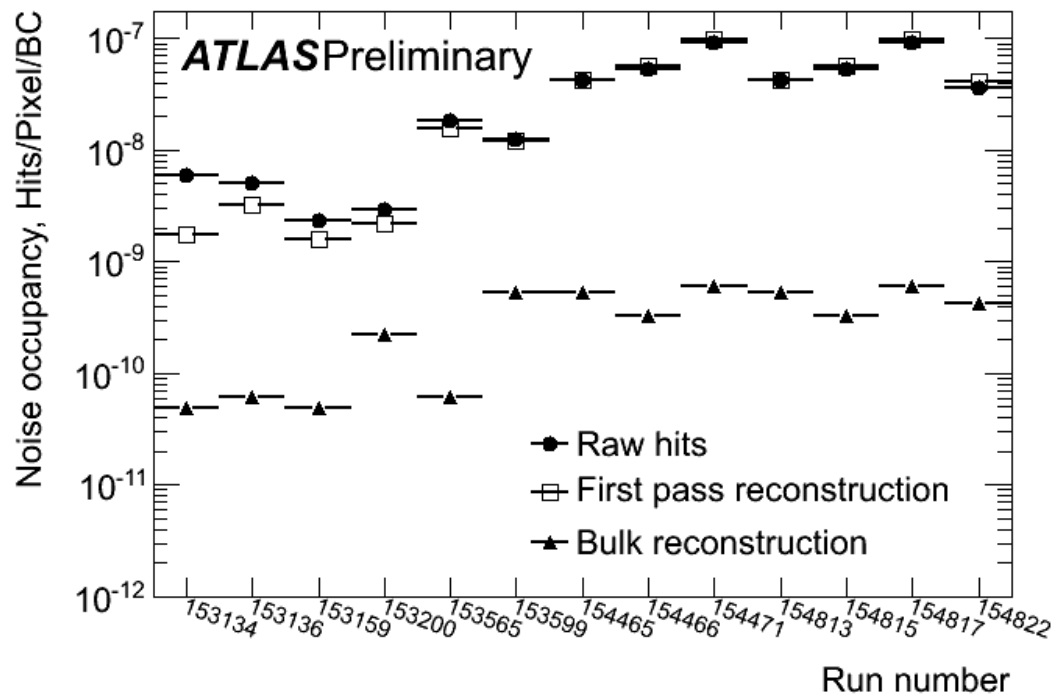
- reconstruction of bulk of data

• Dedicated calibration stream:

- random trigger on empty LHC bunches
- 10 Hz rate
- 29 kB/event

• Express stream:

- ~10 Hz of physics trigger



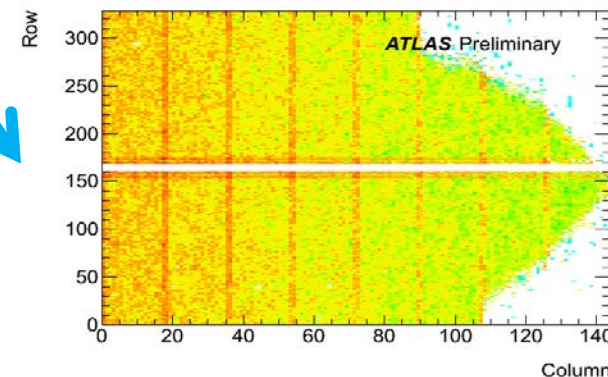
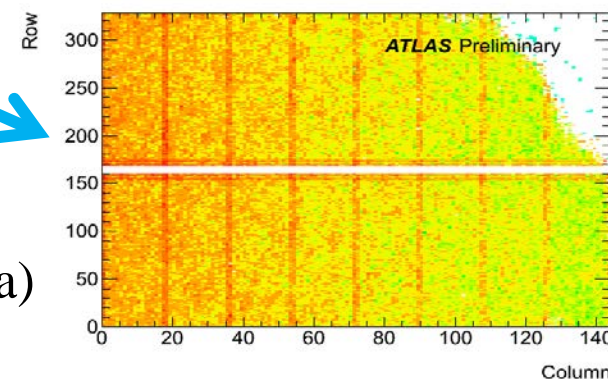
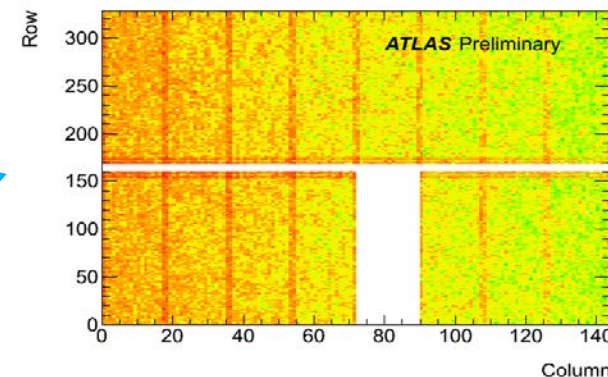
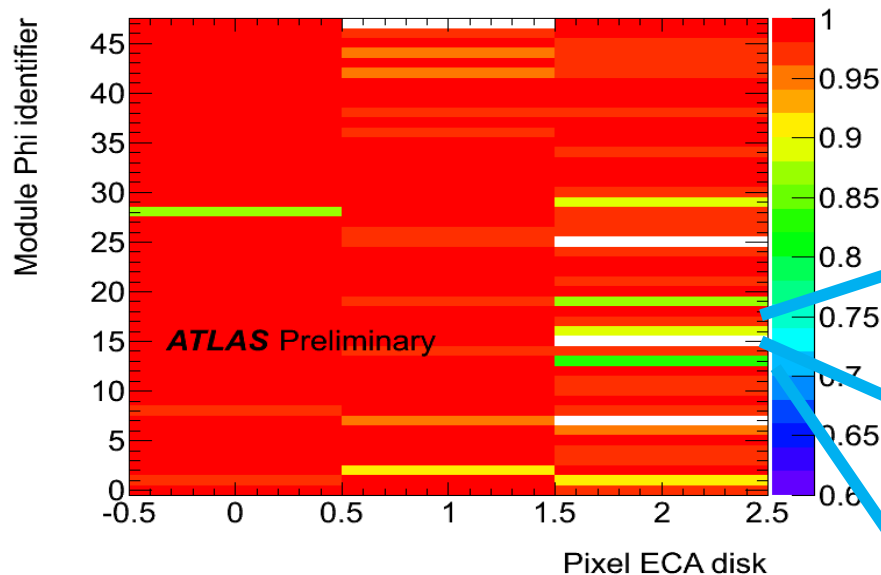
- Mask noisy channels from reconstruction:
 - occupancy $> 1-5 \times 10^{-5}$ hit/BC
 - typically 300-1500 channels masked offline

• Noise rate in bulk reconstruction

- < 0.2 hits/event
(compared to few hundreds in collisions)



Sources of inefficiency

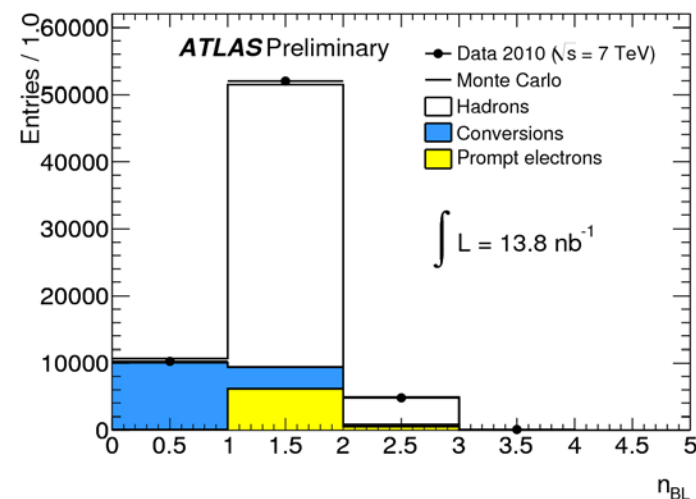
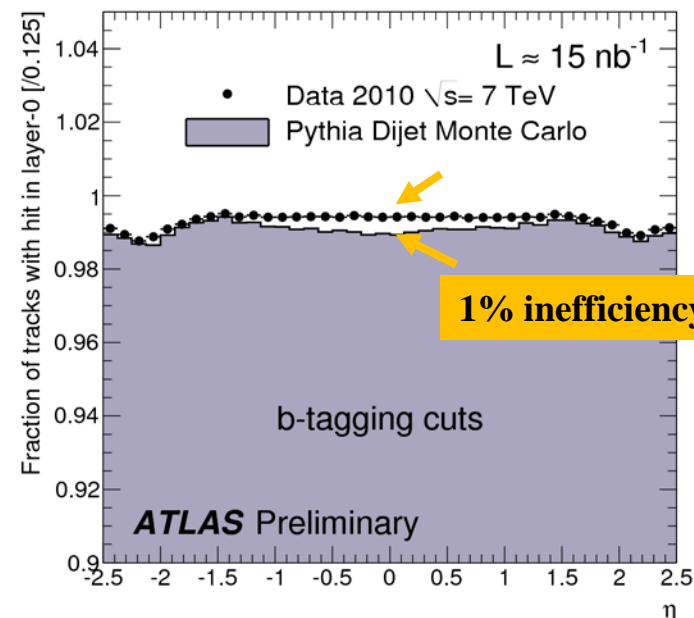


- **Permanent non-operational modules (55/1744)**
- **Temporary non-operational modules (monitored on data)**
- **Maps of inefficient channels:**
 - Dead FE chips (47/27904)
 - Defective bump bonds
 - Bad channels (failing calibrations/disabled online)
- **Very stable with time:**
 - ~260k channel (0.3%)
 - About 50% due to FE failures



Where efficiency matter most!

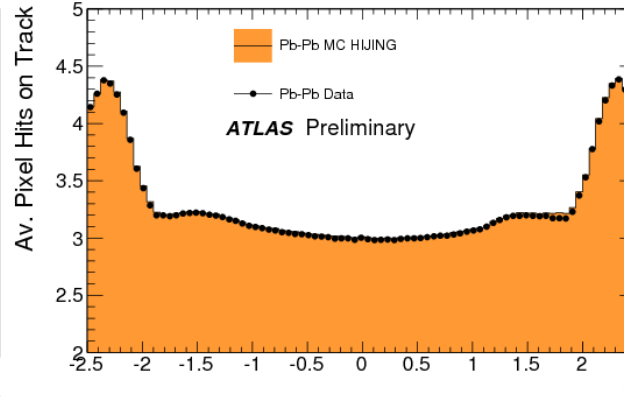
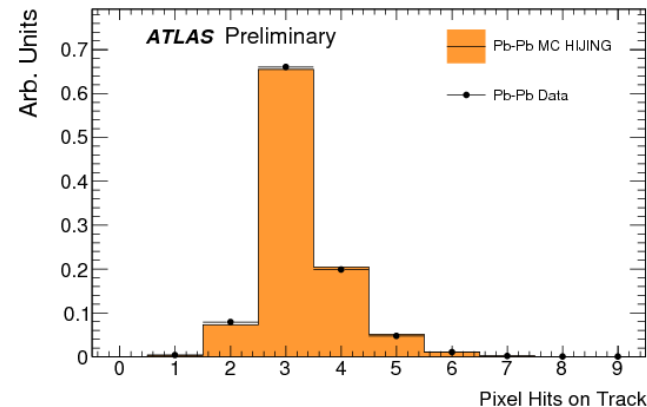
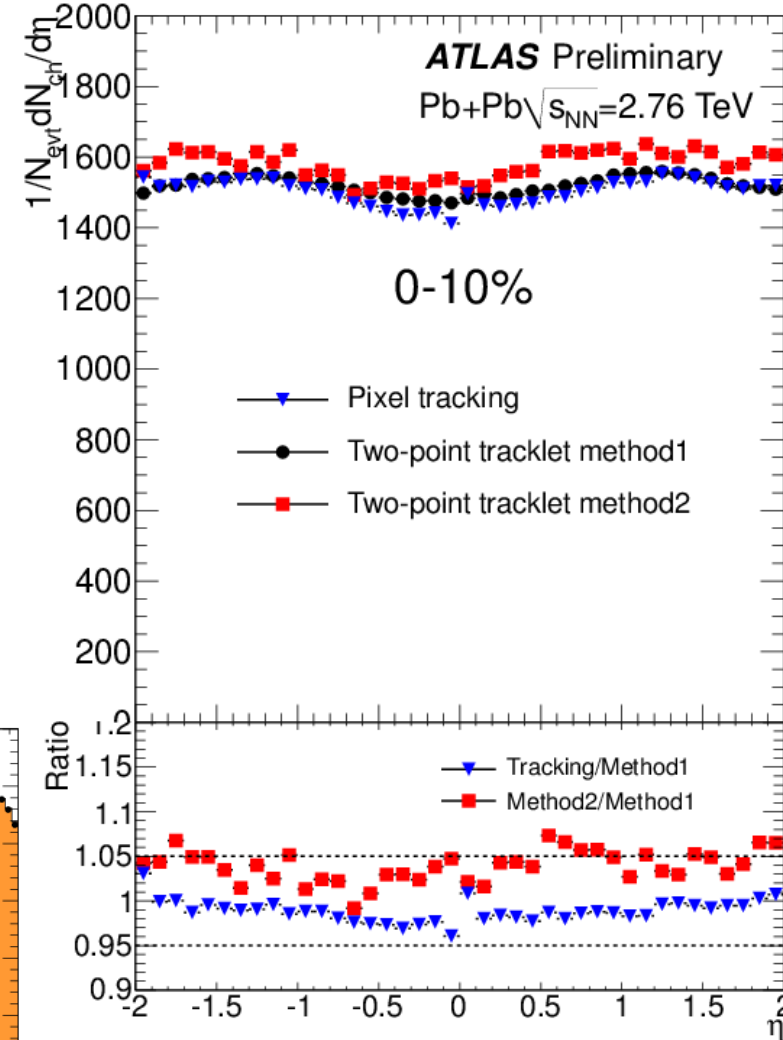
- Intrinsic efficiency measured with cosmic rays and in test beams **almost 100%**.
- This is also confirmed in operation.
- Innermost layer is most critical:
 - Impact parameter resolution is significantly worse is lowest R measurement is missing.
 - It is effectively use to discriminate primary and secondary particles:
 - e/γ separation
 - Soft-QCD studies
 - Heavy-ion reconstruction





Heavy-Ion performance

- To reduce fake tracks in busy HI environments (~ 10000 tracks) no “holes” allowed in Pixel Detector
 - Correct mapping of inefficiency is critical
- Pixel-only tracking powerful for counting very low momentum tracks:
 - **3-points** tracks
 - **Vertex+2-points** tracks
 - Very different efficiency correction.
- **Excellent modeling in simulation.**





Calibration of charge interpolation

Width of track-hit residuals

...and how to make an *hadrography* of the detector

RESOLUTION



Charge sharing

- Point resolution can be improved using the pulse height measurements.

- **Charge sharing variables:**

$$\Omega_x = \frac{Q_{\text{last row}}}{Q_{\text{first row}} + Q_{\text{last row}}}$$

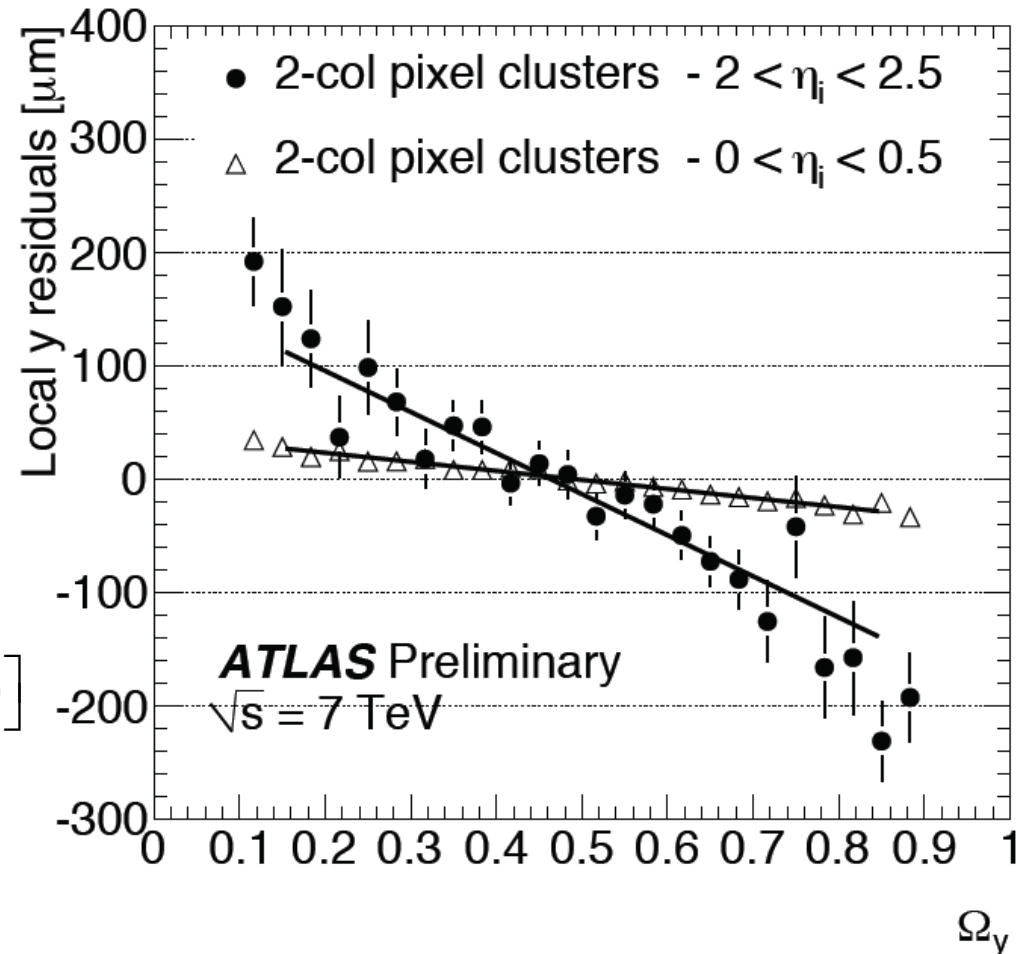
$$\Omega_y = \frac{Q_{\text{last column}}}{Q_{\text{first column}} + Q_{\text{last column}}}$$

- **Cluster position correction:**

$$(x_c, y_c) \rightarrow$$

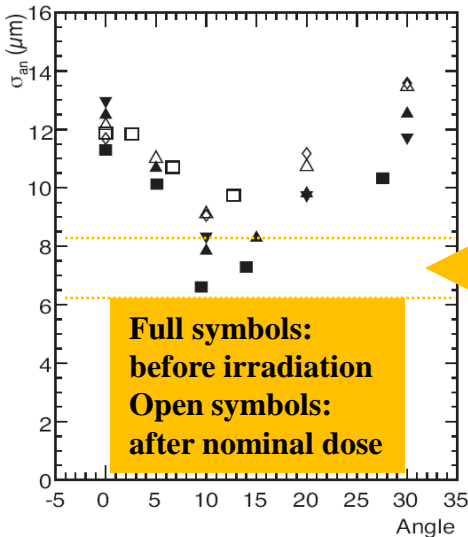
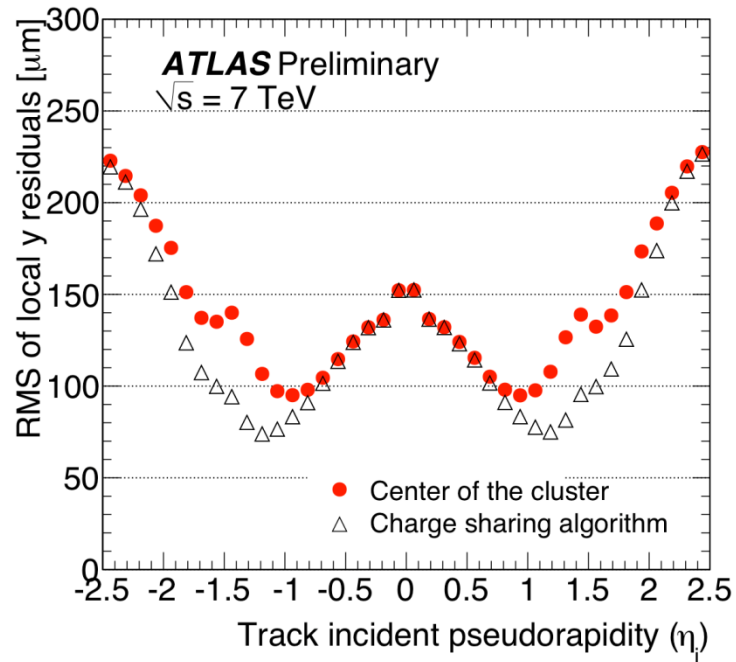
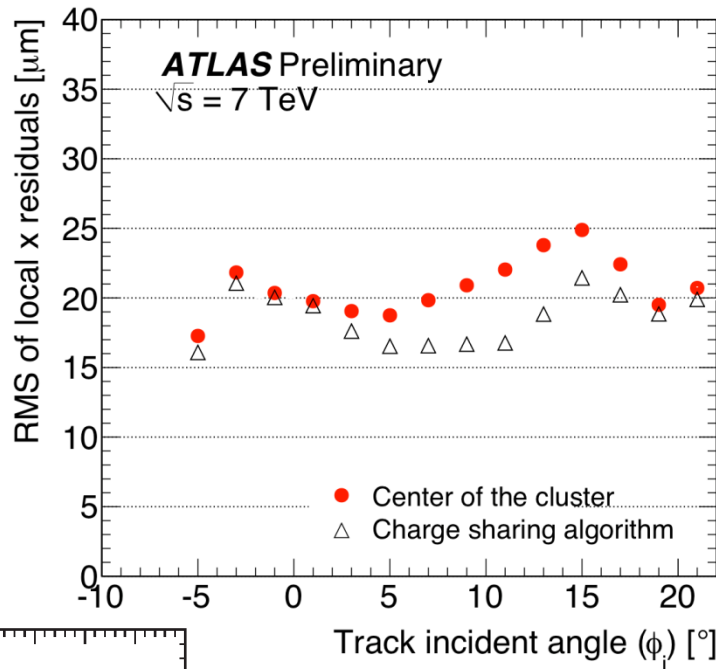
$$\left[x_c + \Delta_x (\Omega_x - 1/2), y_c + \Delta_y (\Omega_y - 1/2) \right]$$

- The parameters Δ_x, Δ_y :
 - depend on cluster size and incident angle
 - **determined from dependence of uncorrected residuals on Ω_x, Ω_y**





Charge sharing: resolution



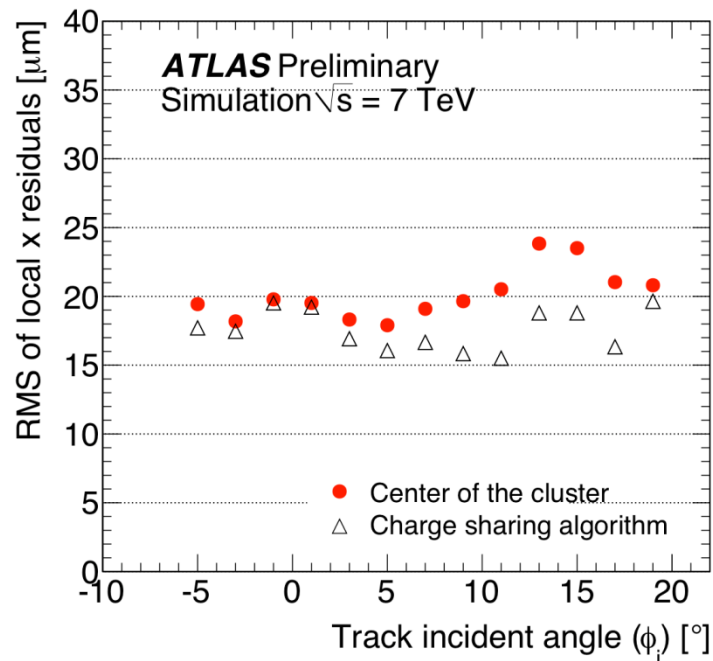
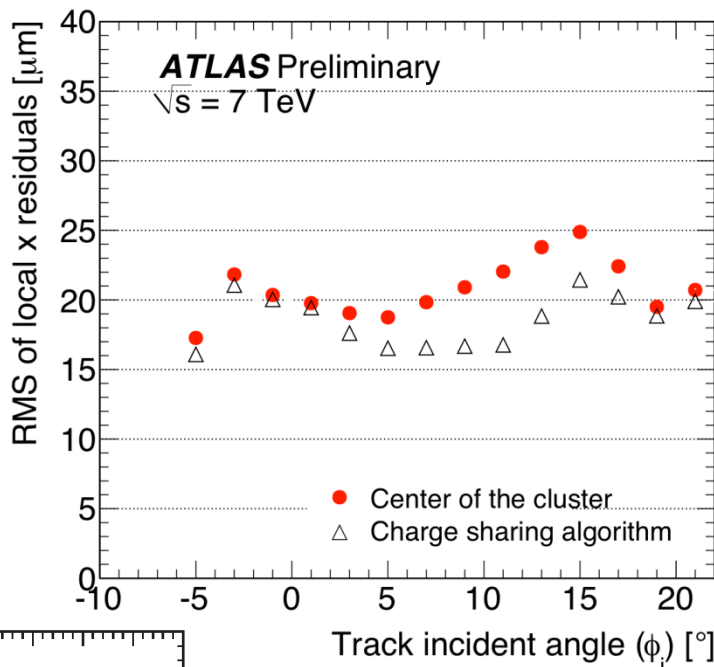
Clear improvement in the angular region populated by 2-pixel clusters.

From test beam studies intrinsic resolution 6-8 μm , before radiation damage

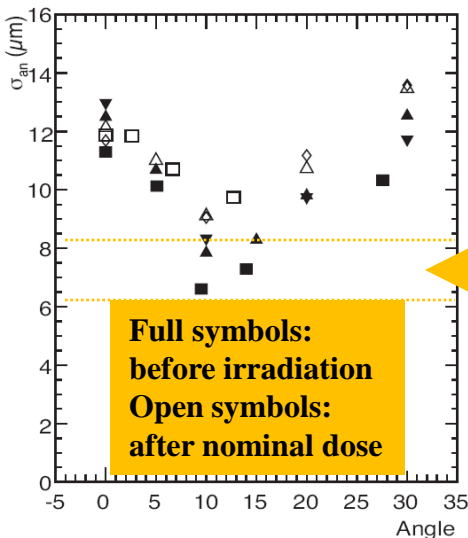
N.B.: residuals include also extrapolation resolution



Charge sharing: resolution



Good agreement with simulation



Clear improvement in the angular region populated by 2-pixel clusters.

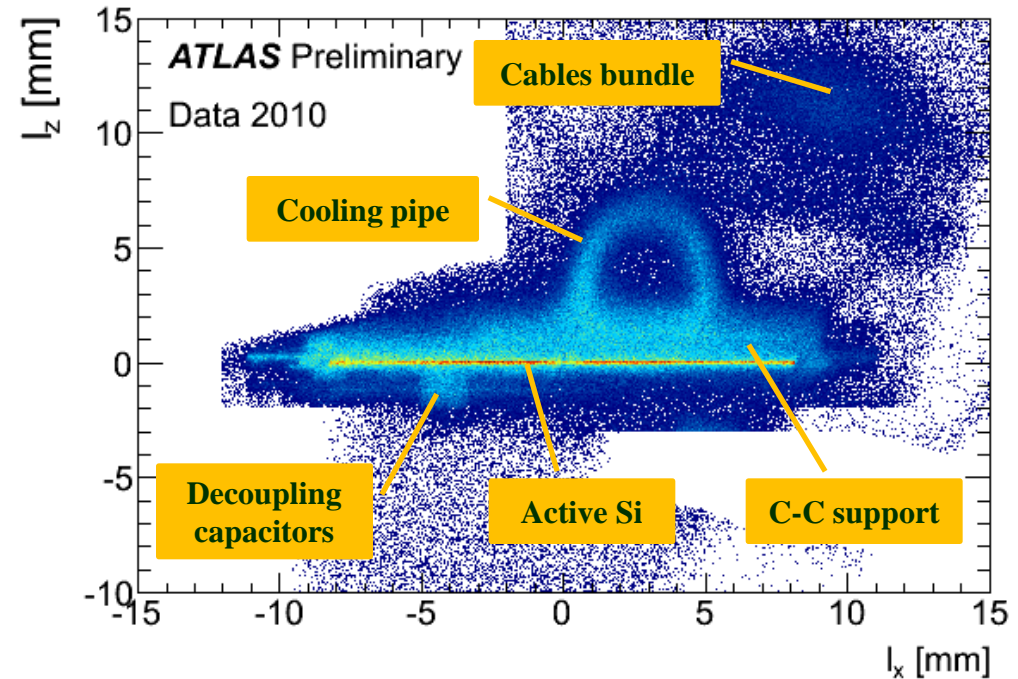
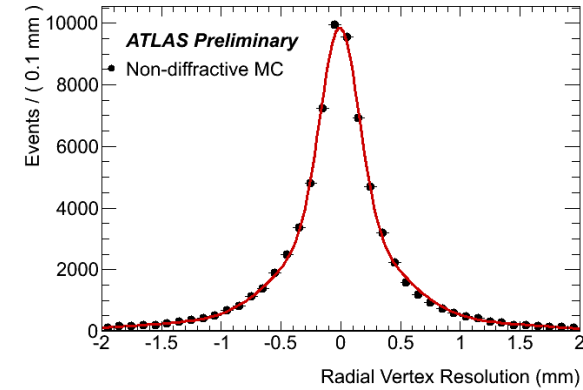
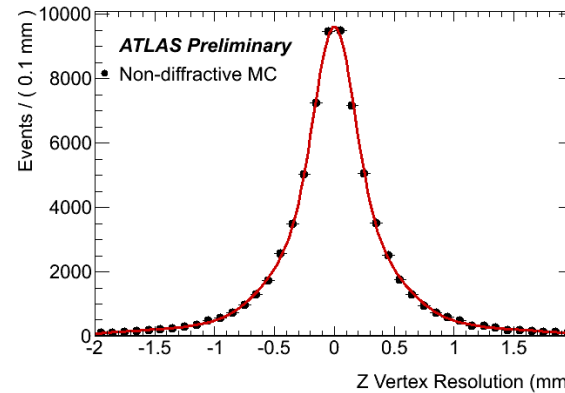
From test beam studies intrinsic resolution 6-8 μm , before radiation damage

N.B.: residuals include also extrapolation resolution



Hadro-graphy

- Material mapping usually performed by photon conversions
- Hadronic interactions can reach a better position resolution:
 - larger opening angle
 - $\sigma=160 \mu\text{m}$ at Layer-0
- Very accurate detector mapping!
- Applications:
 - Average λ_I measurement
 - Positioning of non-sensitive material (beam pipe, support structures)





- Lorentz angle
- Energy loss measurement

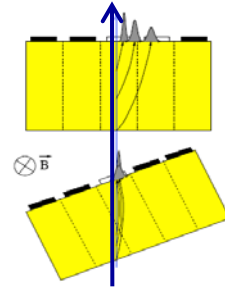
DETECTOR PROPERTIES



Lorentz angle

- Drift in silicon is affected by $E \times B$ effect
- Charge is (de)focused along the Lorentz angle direction:

$$\tan \alpha_L = \mu_H B$$



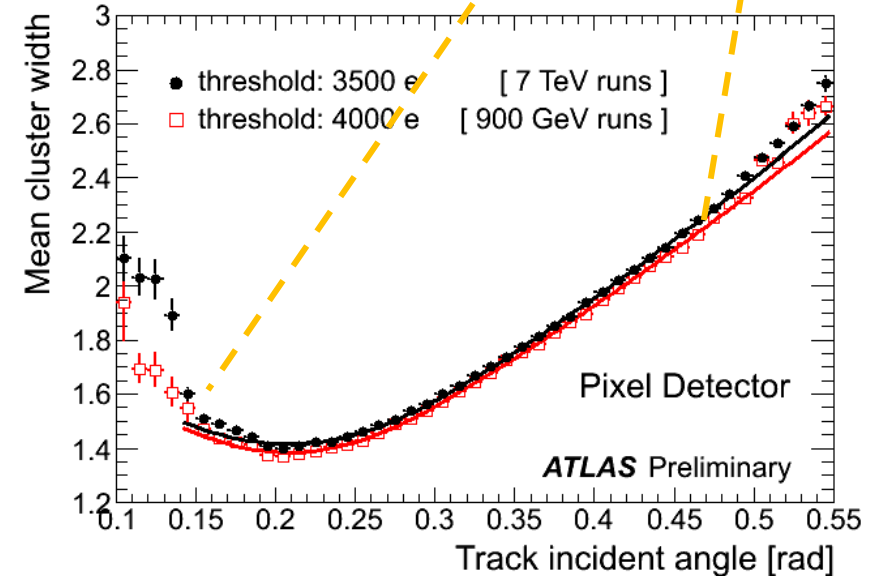
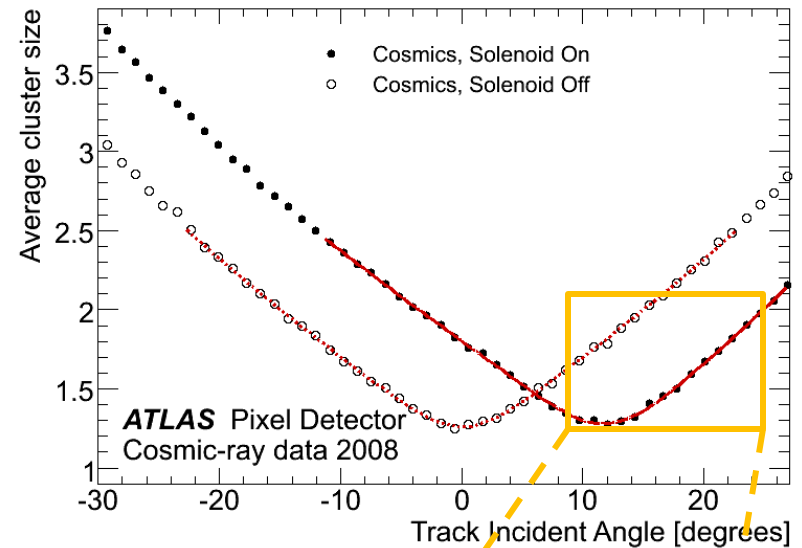
- Point displacement $\approx 30 \mu\text{m}$ for pixels
- **Measurement using cluster size vs. incidence angle α :**

$$\text{cluster size} = a(\tan \alpha - \tan \alpha_L) + b / \sqrt{\cos \alpha}$$

Data sample	α_L [°]
Cosmic rays	$11.77 \pm 0.03^{+0.13}_{-0.23}$
$\sqrt{s} = 900 \text{ GeV}$	12.12 ± 0.15
$\sqrt{s} = 7 \text{ TeV}$	12.11 ± 0.09

Preliminary, only stat. uncertainty

- **Difference due to temperature!**





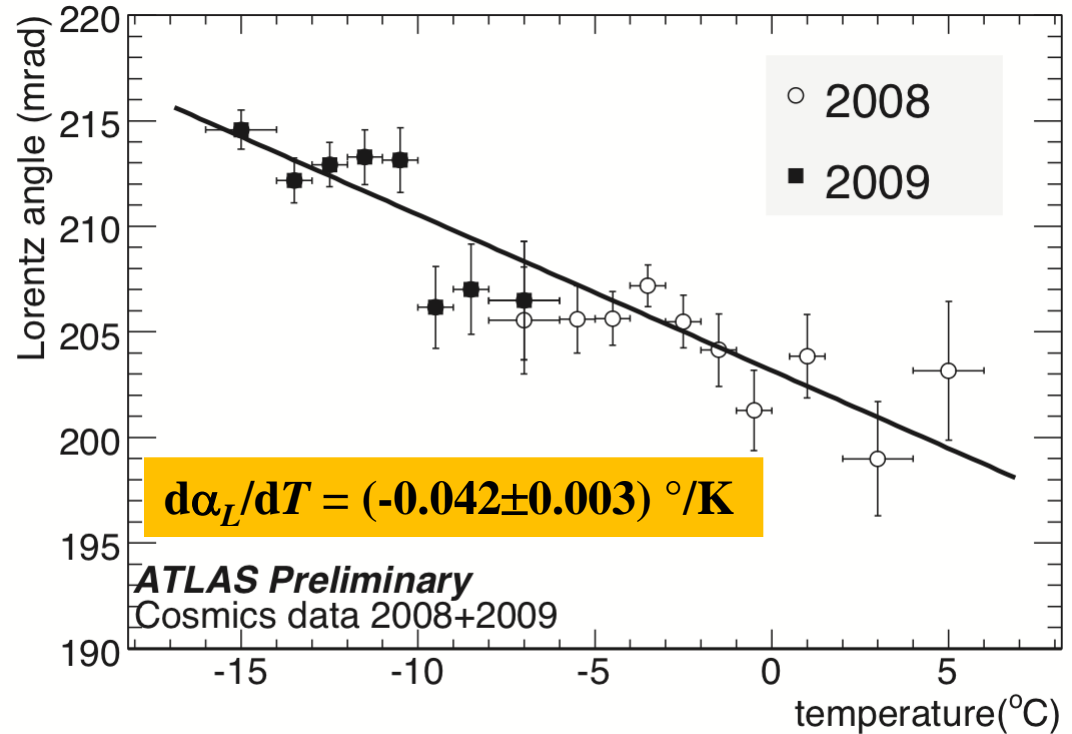
Lorentz angle: T dependence

- The cooling system was commissioned in 2008.
- Since 2009 operation at nominal settings.
- The different operational point allows to measure T dependence of Lorentz angle

$$\tan \theta_L = \mu_H B$$

$$\mu_H = \frac{rv_s / E_c}{\left(1 + (E / E_c)^\beta\right)^{1/\beta}}$$

	Electrons
v_s (cm s ⁻¹)	$1.53 \cdot 10^9 \cdot T^{-0.87}$
E_c (V cm ⁻¹)	$1.01 \cdot T^{1.55}$
β	$2.57 \cdot 10^{-2} \cdot T^{0.66}$
r	$1.13 + 0.0008 \cdot (T - 273)$



Expected from parameterization: $-0.042 \text{ } ^\circ/\text{K}$
Point correction is small: $\sim 0.1 \text{ } \mu\text{m}/\text{K}$
...but nice it can be observed

Parameterization: C. Jacoboni *et al.*, Solid-State Electronics 20 (1977) 77-89.
 T. Lari, ATL-INDET-2001-004



Specific energy loss measurement

- ToT charge measurement well modeled by MC simulation:

- from cosmic ray data:

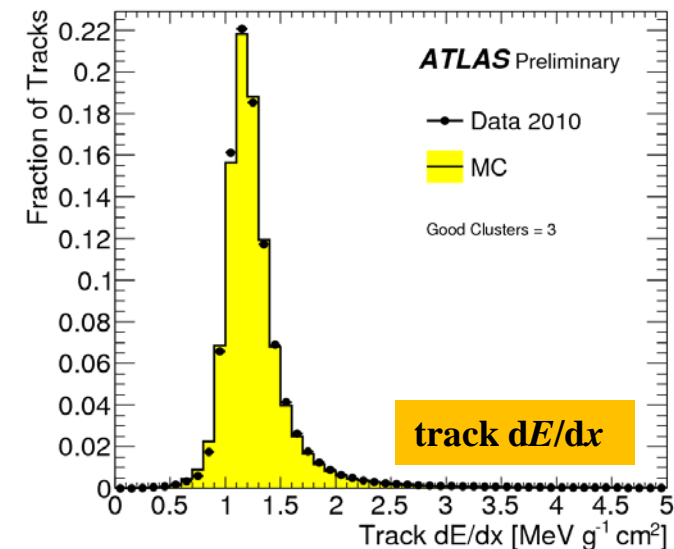
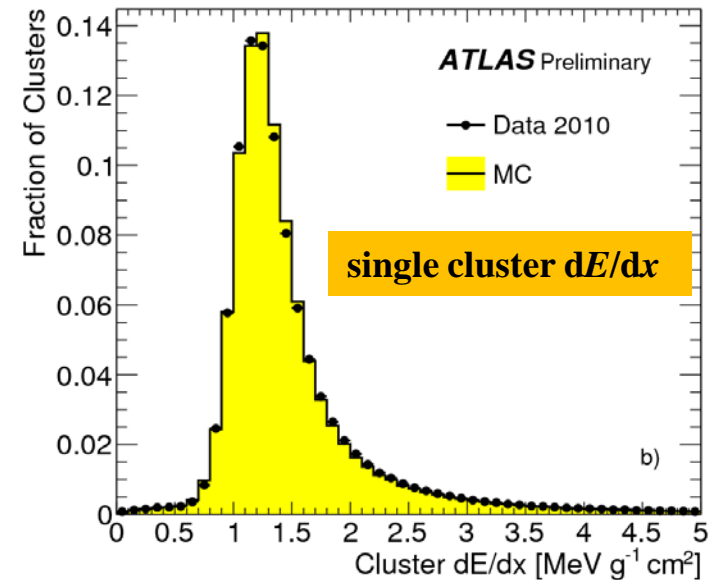
$$\frac{Q_{\text{data}}}{Q_{\text{MC}}} = 0.986 \pm 0.002 \text{ (stat.)} \pm 0.030 \text{ (syst.)}$$

- Since typically a track has three pixel hits, they can be combined to provide a dE/dx measurement:

- remove clusters near module edges or in the ganged region;
- use truncated mean, discarding the cluster with highest energy deposit.

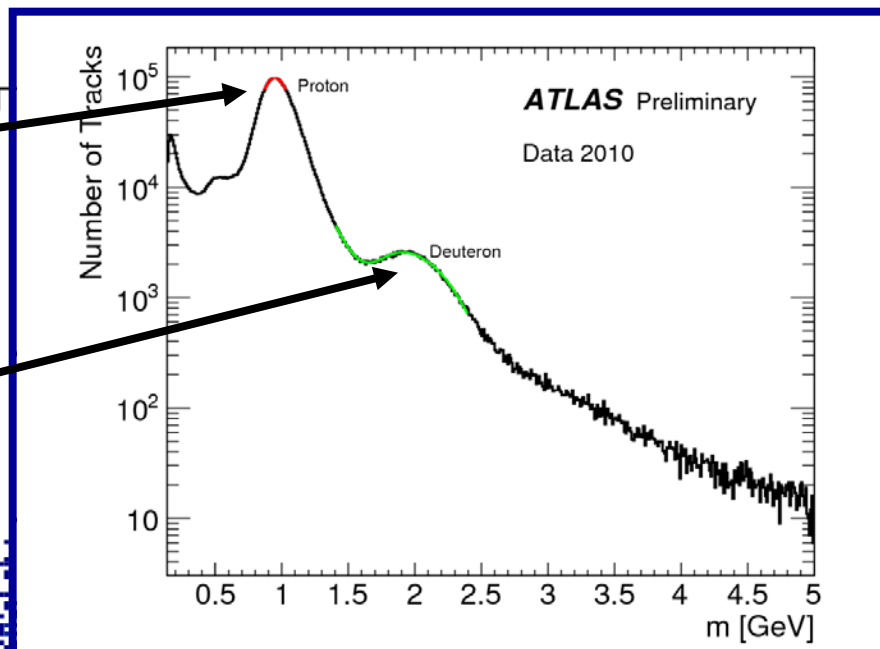
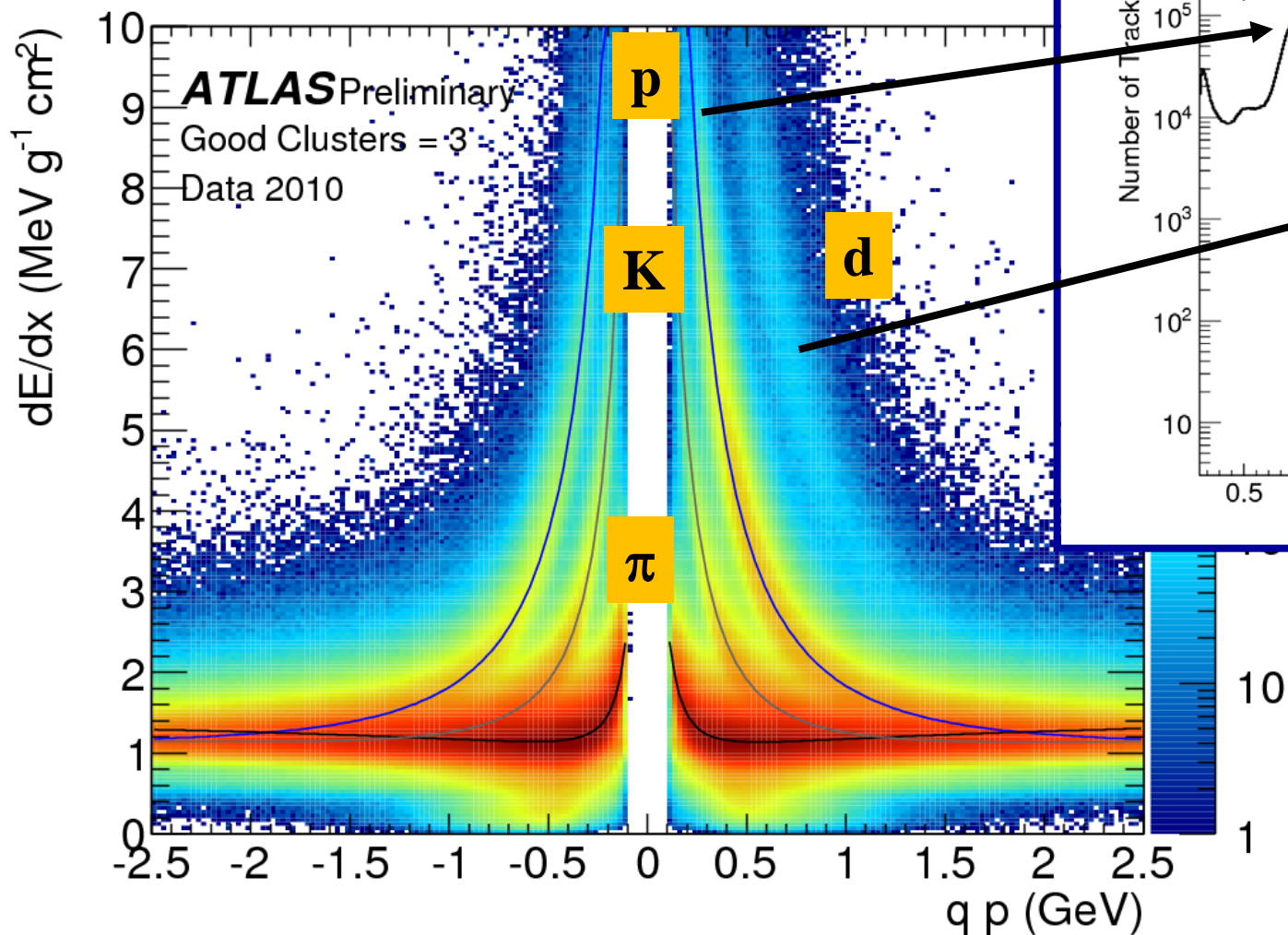
Suppress most Landau tails.

- Resolution of 11% measured on the relativistic plateau





dE/dx at work



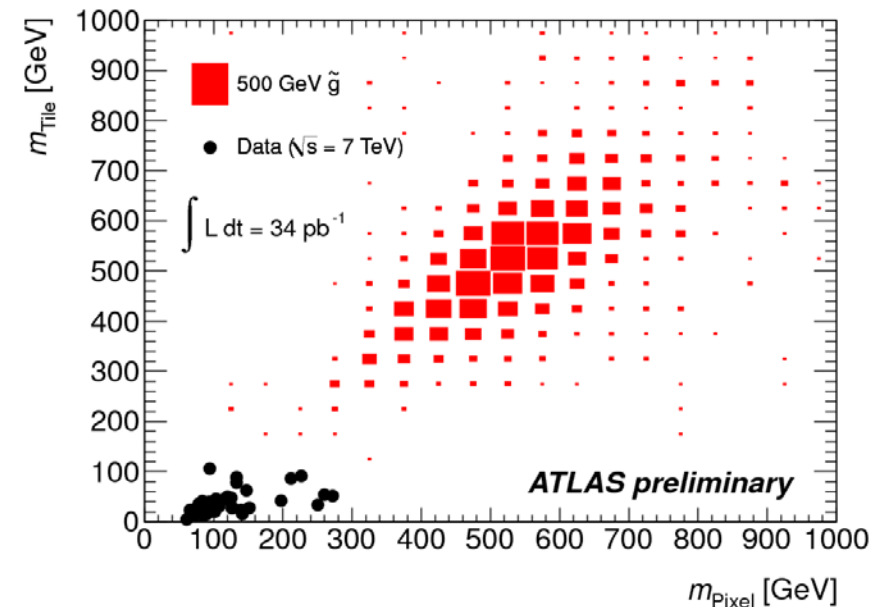
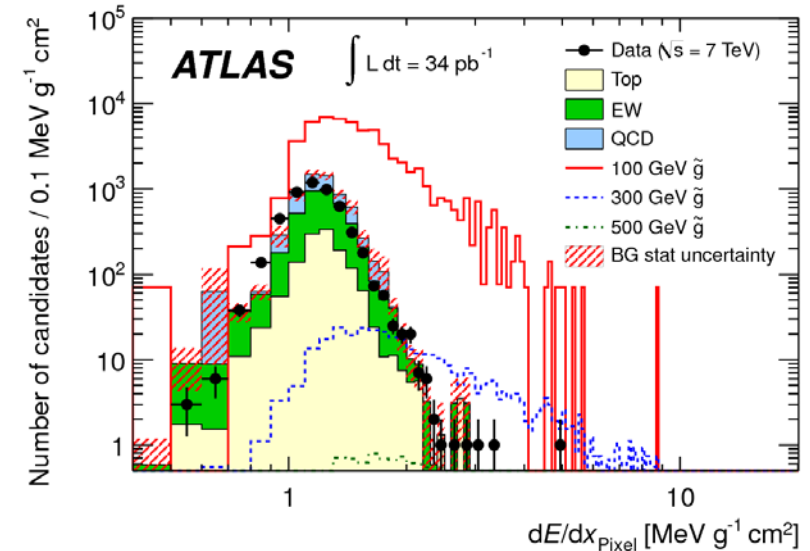
Mass determination inverting
Bethe-Bloch energy loss relation



Applications: R-hadron searches

- Direct application of dE/dx measurement is the search for new particles:
 - **high mass**
 - **long-lived**
 - **charged**
- Example: **R-hadrons**
 - **colourless** states predicted in some SUSY models, composed by stable **squarks** and **gluinos** and ordinary particles
- **Signature:**
 - High- p_T tracks with high energy loss
 - Combination with time-of-flight measurement by calorimeters.
- **Exclusion limits at 95% CL:**

$m_{\tilde{b}}$	>	294 GeV
$m_{\tilde{t}}$	>	309 GeV
$m_{\tilde{g}}$	>	562 GeV





Conclusions

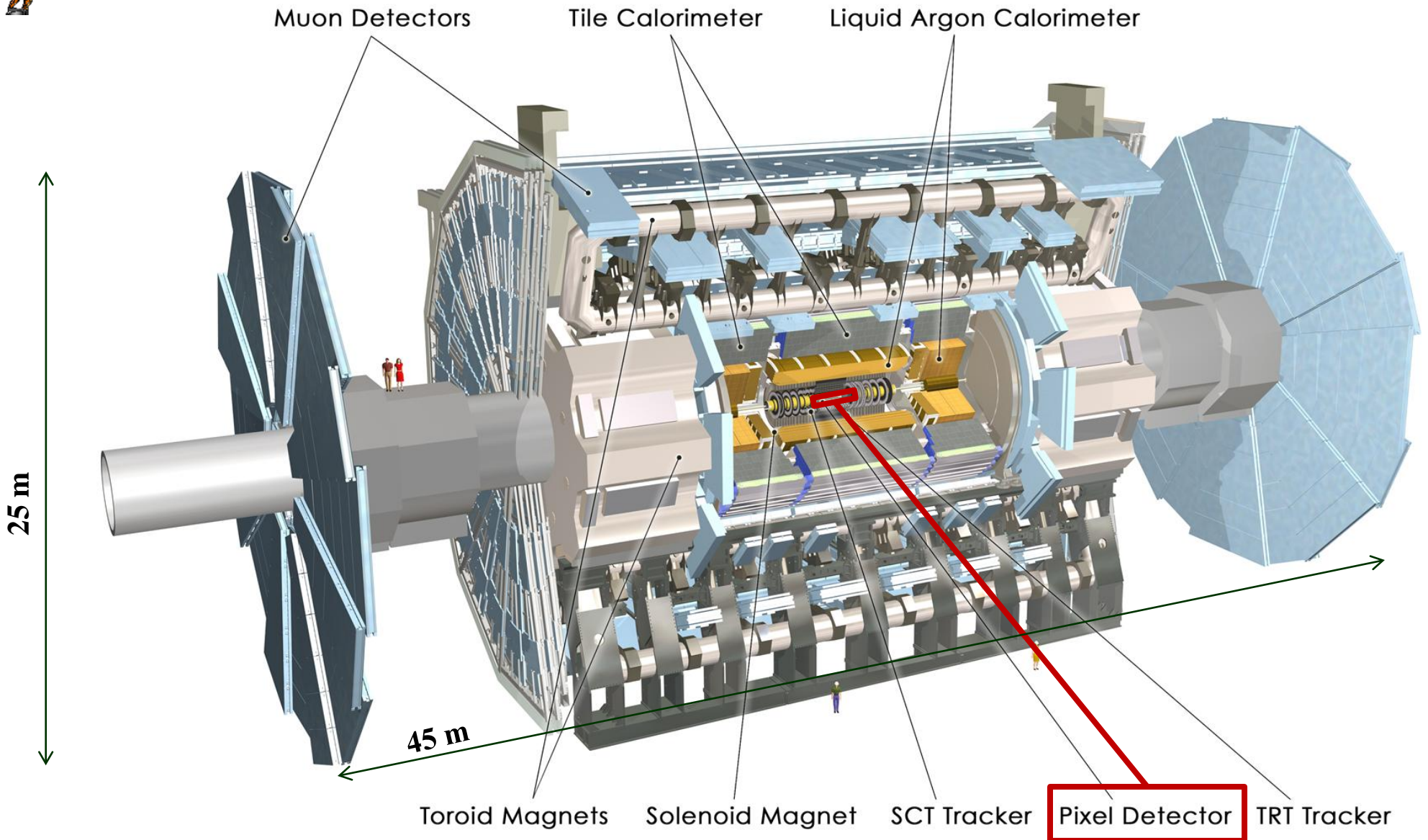
- **Full detector characterization performed:**
 - Mapping of inefficiencies
 - Calibration of charge sharing
 - Lorentz angle measurement and its temperature dependence
 - dE/dx measurement with 11% resolution
 - Material estimation
- **Excellent performance:**
 - noise occupancy rate $O(10^{-10})$
 - track association efficiency at 99% level
 - Resolution near to nominal
- **Pixels in ATLAS physics publications:**
 - Electron and photons
 - Heavy long-lived charged particles
 - Particle multiplicity in heavy ion collisions



BACKUP

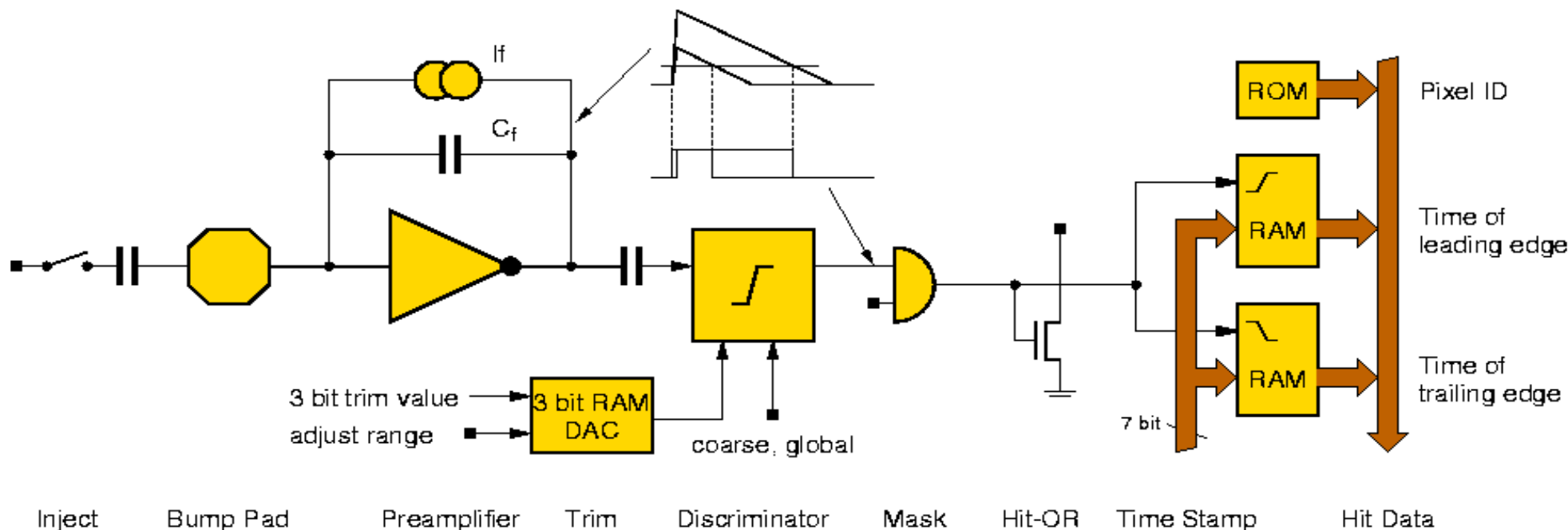


A Toroidal LHC Apparatus





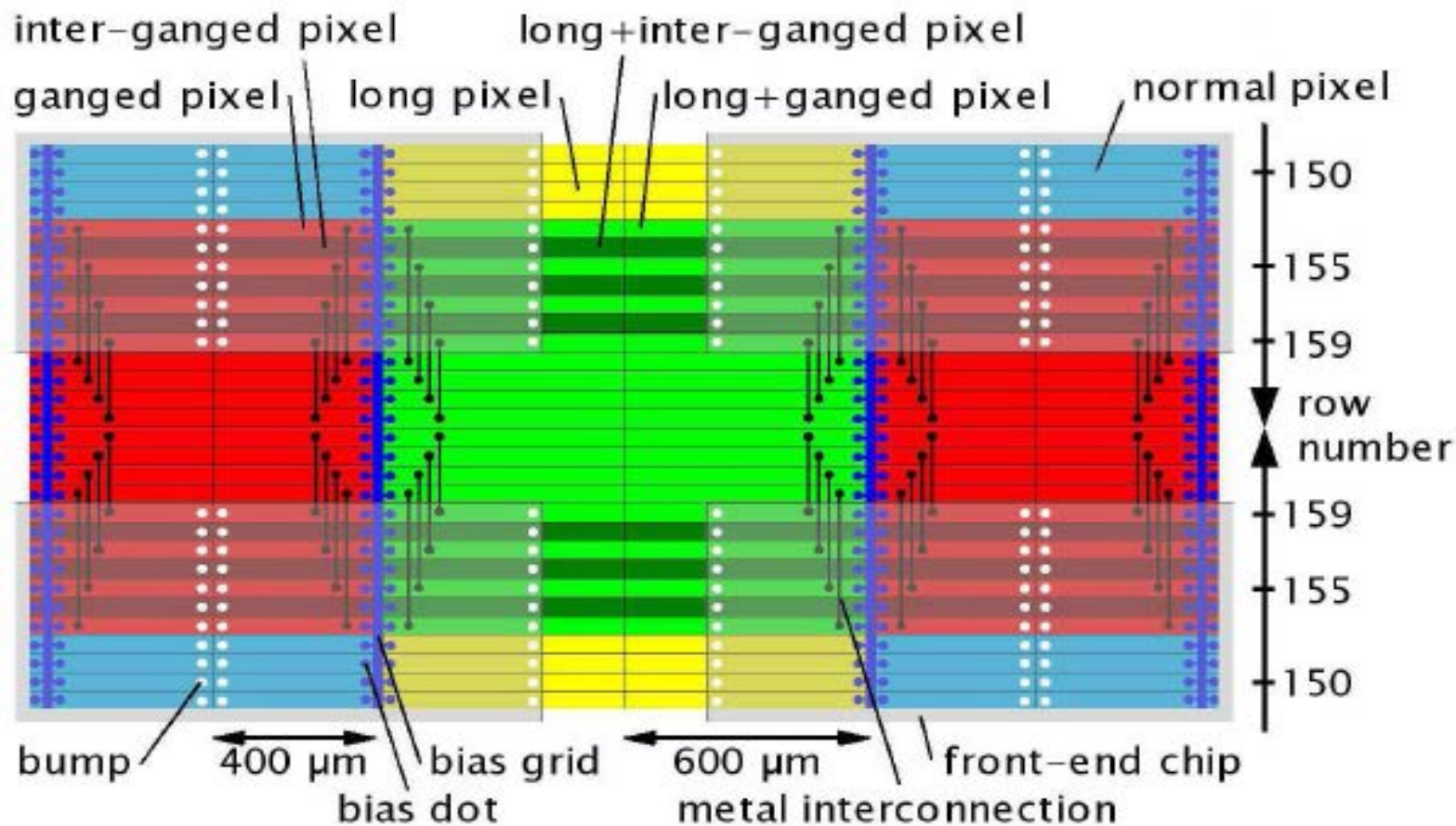
Front-end electronics concept



- Fast charge amplifier with constant current feedback.
- Fast discriminator with tunable threshold (7-bit DAC)
- Storage of hits during the trigger latency time in 64 “End of Column” memory buffers for each column pair of 2×160 pixels



Pixel types

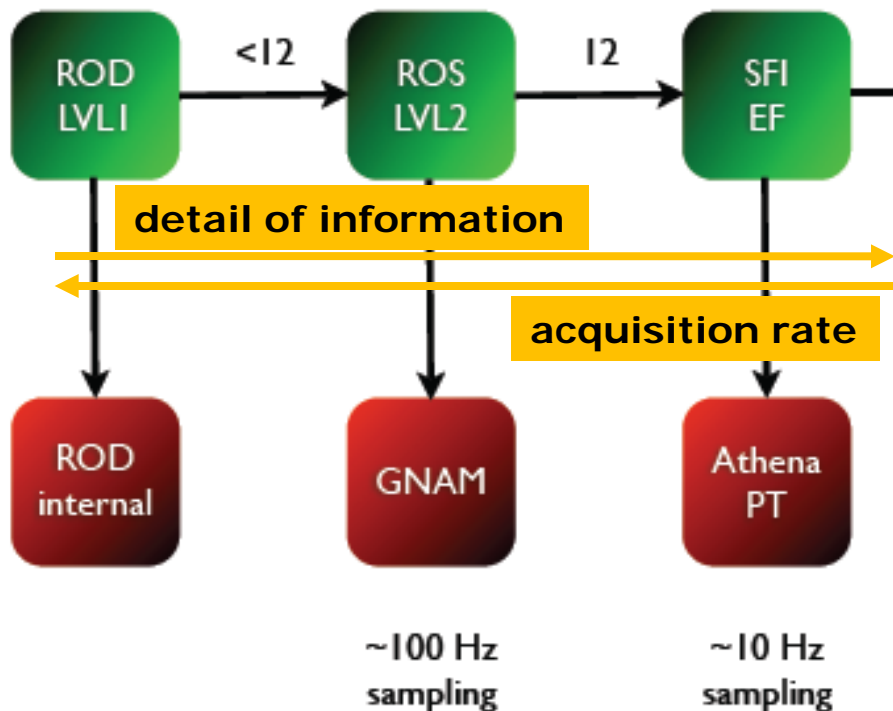


- For ganged pixels, the spacing in the inter-chip region and in the chip-edge regions are different:
for multiple-pixel clusters it is possible to disentangle in which region it was generated.



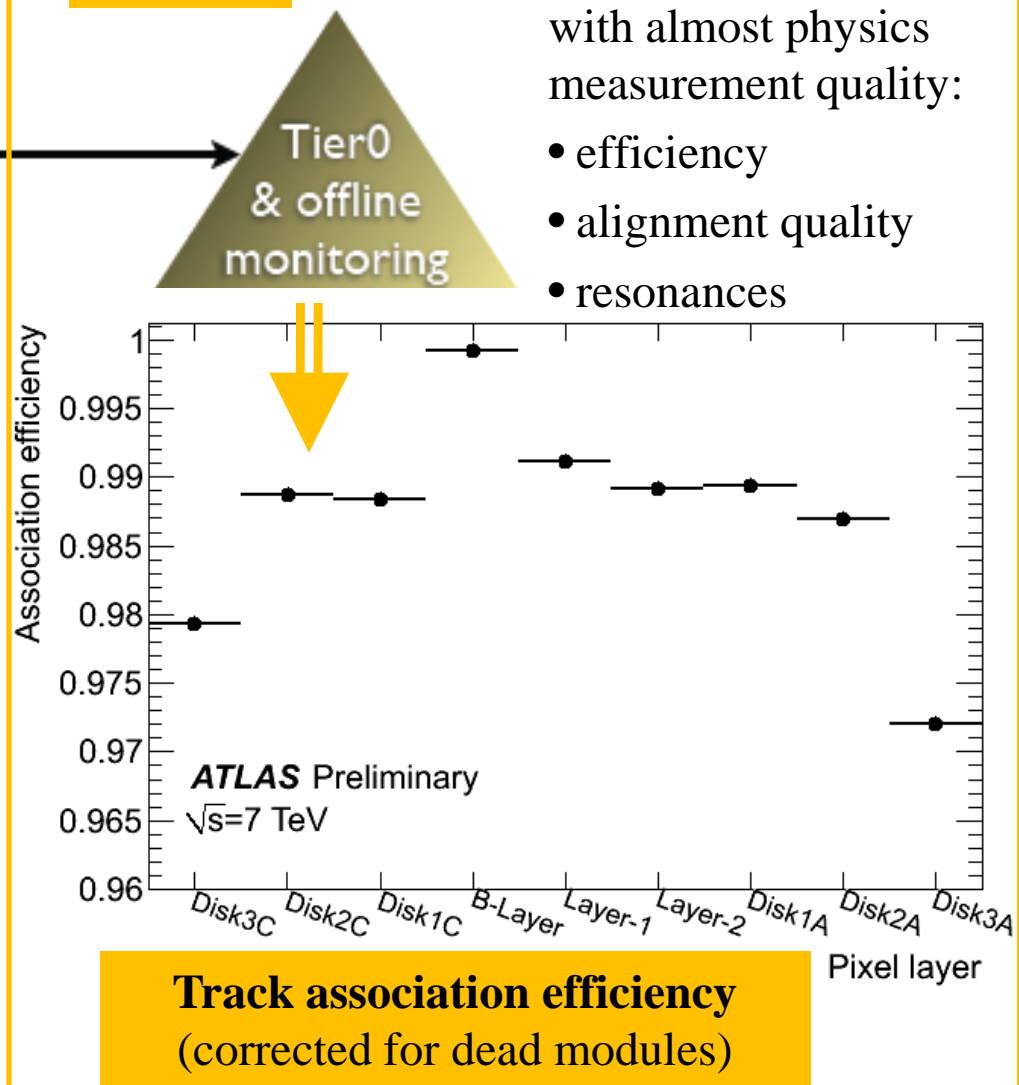
Monitoring

ONLINE



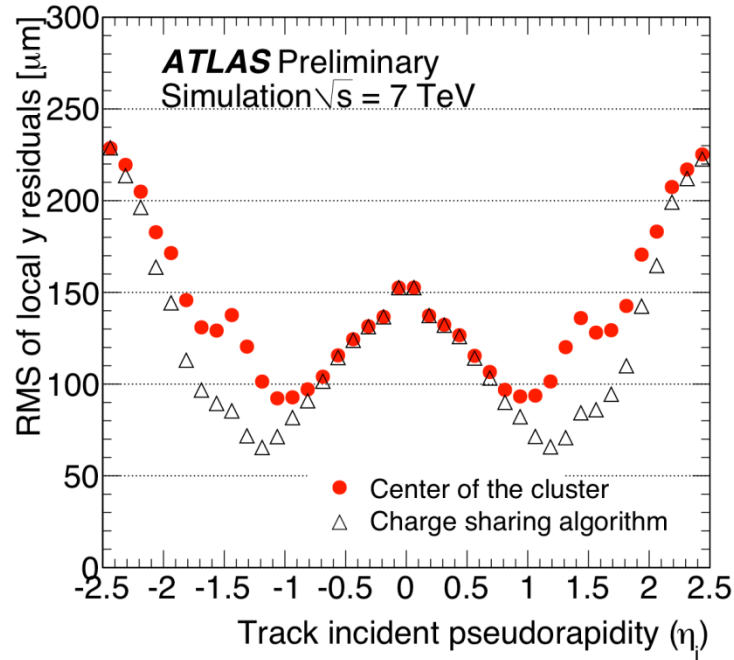
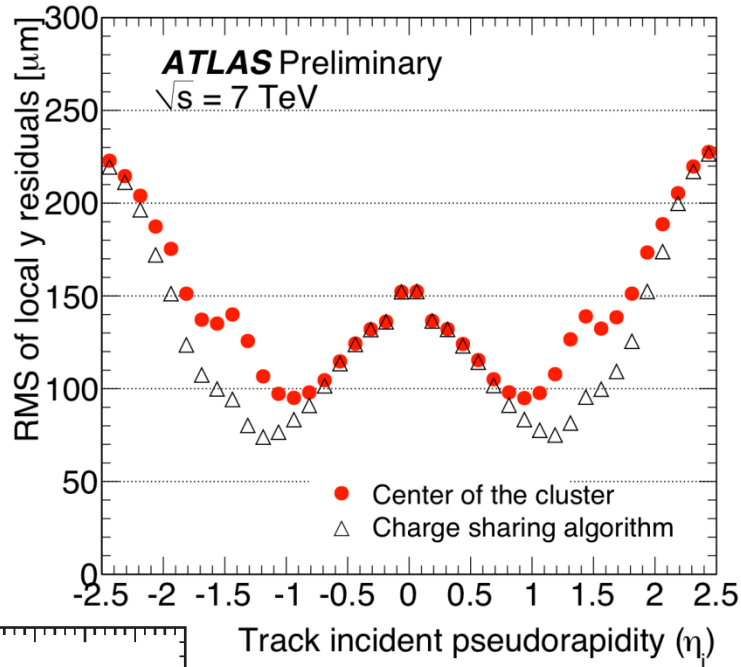
- Occupancy + Disabled modules
- Readout errors + Hit and cluster properties
- ToT distribution + Track reconstruction

OFFLINE

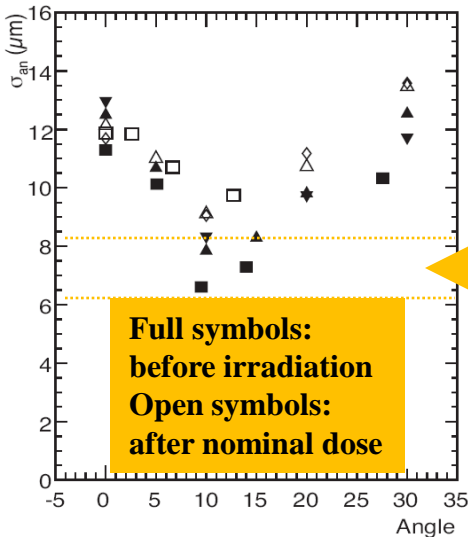




Charge sharing: resolution



Good agreement with simulation



Clear improvement in the angular region populated by 2-pixel clusters.

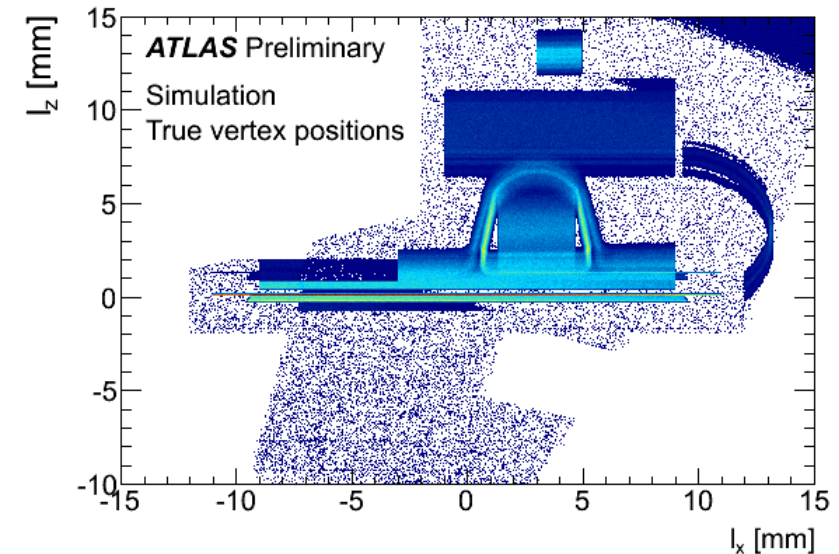
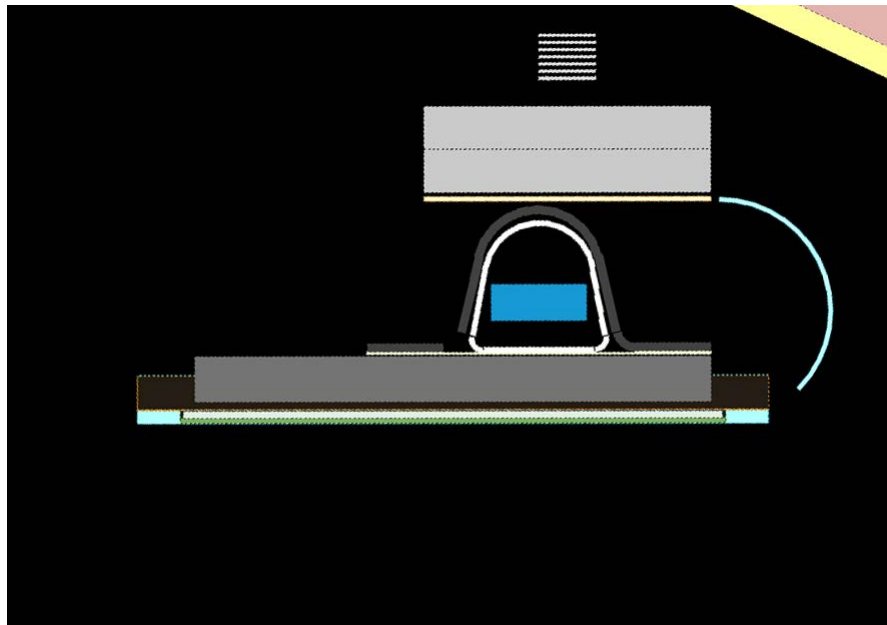
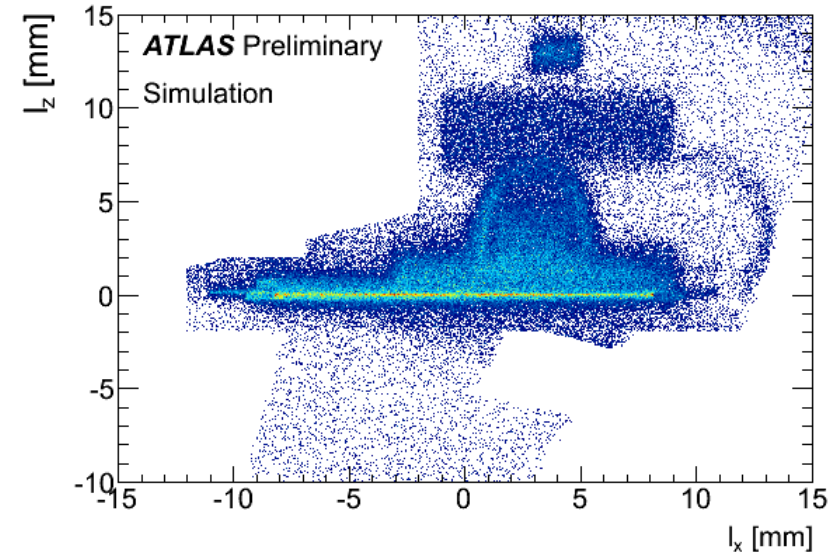
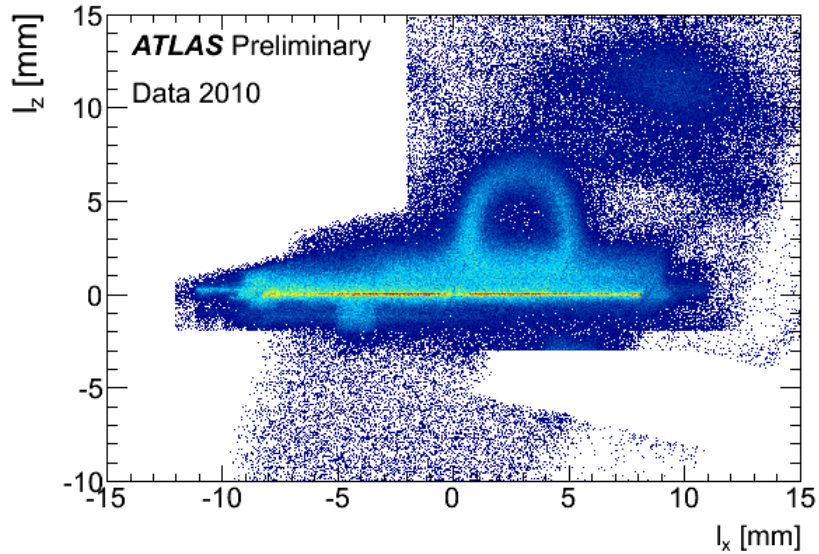
From test beam studies intrinsic resolution 6-8 μm , before radiation damage

Unfortunately residuals include also extrapolation resolution:

in minimum bias collisions dominated by multiple scattering term.



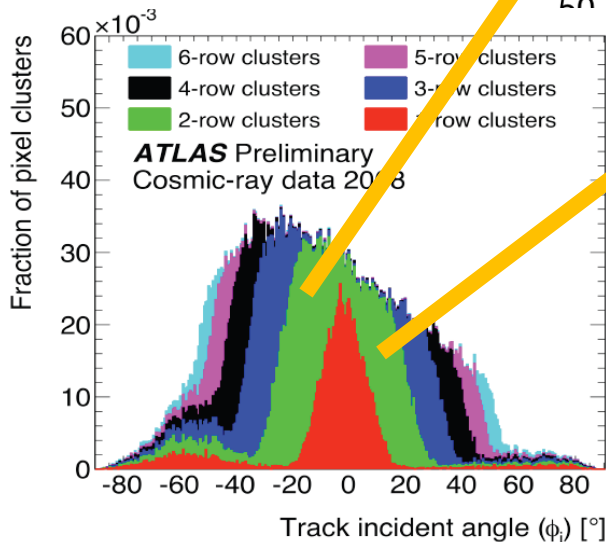
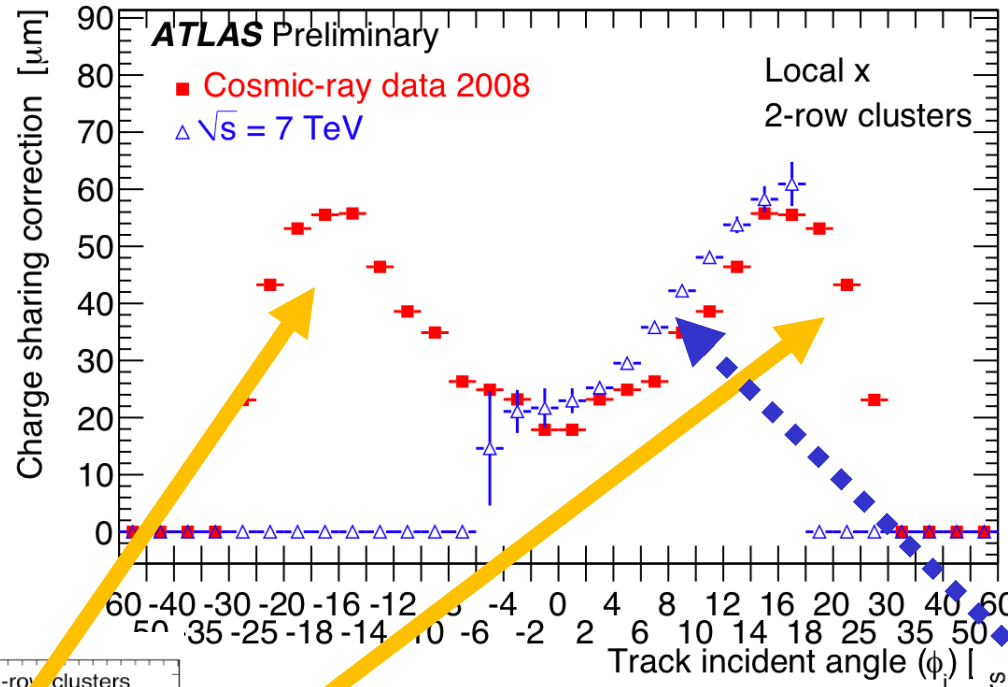
Hadronic interaction maps



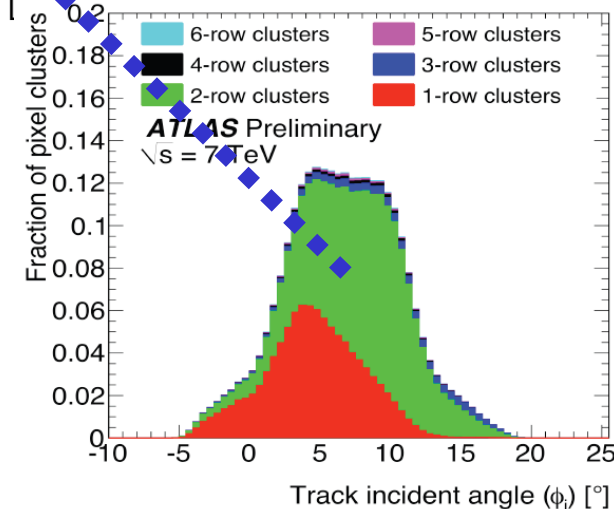


Charge sharing (2)

Δ_x for 2-hit clusters



N.B.: different thresholds used for cosmic rays and collision data

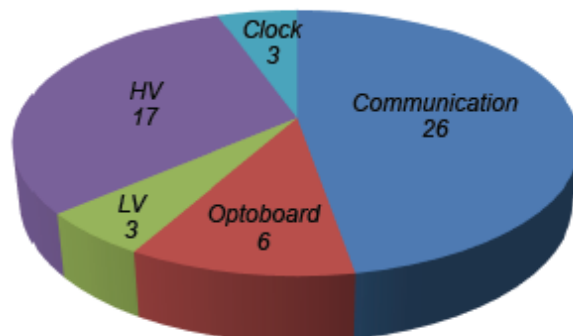




Pixel Detector Status

- 96.8% of the detector active in data taking
 - 55 Modules disabled (3.2%)
(6 modules due to a single opto-board failure)
 - 47 FE chips disabled (0.16%)
 - In particular failures are linked to thermal cycles
 - an attempt has been made to reduce the problem by smaller temperature variations with first modest results, more refinements will be tried
 - The percentage of disabled modules grew from 2.1% to 3.2% in 3 years of operations

Disabled modules by failure type:



Inactive fraction per layer:

B-layer	3.1 %
Layer 1	1.4 %
Layer 2	4.6 %
Endcap A	2.8 %
Endcap C	2.8 %

